Enhancing the Kramers-Kronig Receiver via Dispersion-Based Spatial Diversity

LIOR BLECH[1], CRISTIAN ANTONELLI[2], ANTONIO MECOZZI[2], YONINA C. ELDAR[3], AND MARK SHTAIF[1]

[1] School of Electrical Engineering, Tel Aviv University, Tel Aviv 69978, Israel
[2] Dept. of Physical and Chemical Sciences, University of L'Aquila, 67100 L'Aquila, Italy
[3] Department of Mathematics and Computer Science, Weizman Institute of Science, Rehovot, Israel
[*] Corresponding author: shtaif@tauex.tau.ac.il

Compiled May 16, 2020

We report a scheme for reconstructing the complex envelope of an optical signal from two decorrelated measurements of its intensity. The decorrelation is achieved by splitting the received optical signal into two copies, and by dispersing one of the copies prior to photo detection. The reconstructed complex-valued signal is obtained by means of an iterative algorithm that requires only a few tens of iterations. The starting point of the search procedure is produced by Kramers-Kronig (KK) reconstruction. With this procedure the continuous-wave tone that accompanies the received signal is reduced by 5 dB to 6 dB compared to the requirement of a KK receiver alone.

http://dx.doi.org/10.1364/ao.XX.XXXXXX

The problem of reducing the cost of fiber-optic transceivers has been challenging the optical communications community in recent years [1–12]. An attractive approach for meeting this challenge has recently been proposed in the form of the Kramers Kronig (KK) receiver [4–12], which is capable of reconstructing complex-valued QAM modulated signals from a simple intensity measurement performed with a single photo-diode. The main idea underpinning the KK-scheme is that a CW tone accompanies the data-carrying signal, such that its frequency is incrementally outside the spectrum of the data-carrying signal, and its power is large enough to ensure that the overall electric field satisfies the minimum-phase condition [4]. The ratio between the CW power and the average power of the data carrying signal is referred to as the carrier to signal power ratio (CSPR), and in typical configurations, assuming 16 QAM modulation, proper operation of the KK-scheme requires a CSPR of approximately 7 dB [4]. While this CSPR is considerably smaller than in other previously reported alternatives [4, 5], it still imposes a non-negligible constraint on the transmitter. Additionally, the presence of such a strong carrier is undesirable from the standpoint of nonlinear fiber-propagation effects, particularly in the presence of multiple-channel transmission, as is done in wavelength-division-multiplexed (WDM) systems.

The fact that the reconstruction of the optical phase of a signal from a measurement of its intensity requires the presence of a sufficiently strong carrier is fundamental, as has been shown in [13, 14]. It is the presence of a carrier that allows the satisfaction of the so-called minimum-phase-condition [4] which guarantees a unique relation between a signal's phase and intensity waveforms. In the absence of a carrier, or when the carrier is insufficiently strong, the received intensity can be matched to multiple phases and the reconstruction of the correct optical phase can no longer be generally guaranteed. A way of circumventing this requirement has been proposed in [15], where the complex envelope of a signal is recovered by means of measuring two decorrelated replicas of the signal's intensity. The intensity-waveform decorrelation is achieved by splitting the received optical signal into two identical copies and passing one of the copies through a known dispersive element prior to photo-detection, as illustrated in Fig. 1. The reconstruction of the complex-envelope of the signal is then performed by numerically searching for a complex waveform that is consistent with both of the measured intensities. Yet, since it is impossible to guarantee neither the uniqueness of an appropriate solution, nor the ability of finding it with a practical search algorithm, the above-described procedure requires additional anchors that ensure the extraction of a correct solution.

In [15], the anchor was provided by applying a KK reconstruction procedure to the intensity that was received in one of the arms, and then using the KK-recovered waveform as an initial condition for the process of searching for the correct solution. Since the KK procedure is only meant to provide an initial condition for subsequent optimization, the CW tone could be considerably smaller than the level that is required for satisfying the minimum phase-condition. Thus, we were able to numerically demonstrate complex signal reconstruction with a 3 dB weaker CW carrier than would be required in a standard KK procedure. For this reason the scheme proposed in [15] was named the enhanced Kramers Kronig (EKK) receiver.

Another interesting approach that has been reported recently, anchors the numerical search procedure by inserting known pilot signals into the transmitted information [16, 17]. The advantage of this approach is that it does not require any CW carrier, but the reliance on pilot symbols introduces its own toll, mostly in terms of complexity and a larger sensitivity to noise (as the pilot symbols need to be recoverable with acceptable reliability). A major issue that is shared by all of the reported

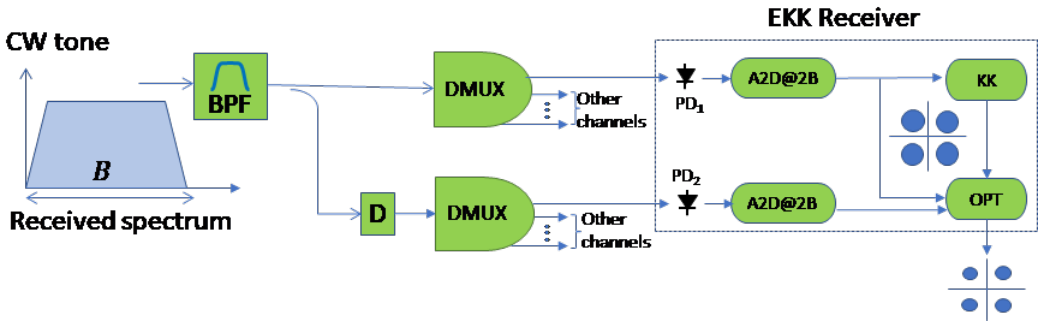

Fig. 1. The proposed EKK scheme. The received signal is split into two replicas, one of which is dispersed, so as to decorrelate the intensity patterns. The KK is used as initial condition for the algorithm.

approaches [15–17] is the relatively large number of numerical search iterations that makes the practical implementation of these methods rather challenging.

In this letter we report major advancements in two of the most important parameters of the EKK receiver. The required CW power that we report here is now nearly 6 dB below the power that is required by standard KK, and even more impressively, the complexity of the optimization procedure was reduced by more than a full order of magnitude. The improvement with respect to [15] was realized by combining the modified gradient expression of [19] with the Polak-Ribiere conjugate gradient method, which produced more efficient convergence.

Figure 1 shows the EKK setup. It consists of an optical filter, followed by a 3dB splitter and a chromatic dispersion module that is inserted in the lower branch in order to decorrelate the detected intensities. The WDM spectra in each of the branches are then separated into individual channels by means of an optical demultiplexer, with two decorrelated replica of each channel entering each EKK receiver. As noted earlier, one of the receiver arms undergoes KK reconstruction, which is crude because the CW carrier is way below what is required in order to fulfill the minimum-phase condition. The KK reconstruction then serves as initial condition for the numeric optimization process that searches for the complex waveform as we elaborate below. Notice that the cost of the additional optical hardware consisting of the dispersive element and of the extra demultiplexer, is expected to be small, as it is shared by all of the WDM channels in the system. In what follows we elaborate on the optimization process and present simulation results for 16-QAM and 64-QAM modulated transmission in the linear and in the nonlinear propagation regimes.

We assume a setting identical to that of the KK scheme [4], where the receiver is preceded by a band-pass optical filter of bandwidth B. Focusing for the time being on the linear propagation regime, the signal impinging on the first and second photo-diodes (PD_1 and PD_2 in Fig. 1, respectively) can be written as

$$E^{(A)}(t) = E_0 e^{i(\pi B t+\phi)} + \sum_k a_k g\left(t-kT\right) + n(t) \quad (1)$$

$$E^{(B)}(t) = E_0 e^{i(\pi B t+\phi')} + \sum_k a_k g'\left(t-kT\right) + n'(t), \quad (2)$$

where a_n are complex-valued data symbols and $g(t)$ is the fundamental pulse waveform including the effect of the link's chromatic dispersion. We will assume that the spectrum of this waveform (typically a raised cosine) is fully contained in $[-B/2, B/2]$ (implying that the angular frequency is within $\omega \in [-\pi B, \pi B]$).

The term E_0 represents the complex amplitude of the CW tone, positioned (as in [4–6]) at the low frequency edge of the received spectrum, and ϕ is the phase delay imposed on the CW tone owing to the link's dispersion. Finally, $n(t)$ is the filtered contribution of the ASE noise. The effect of the dispersive element positioned in the lower arm in Fig. 1 is to modify the phase of the CW tone to ϕ' and to change $g(t)$ and $n(t)$ into $g'(t)$ and $n'(t)$, respectively. While in principle any kind of all-pass filter can be used in the role of the dispersive element, as stated earlier, we assume a dispersive element that produces a quadratic dependence of the phase on frequency, namely equivalent to a standard transmission fiber. Alternatively, any commercially available dispersion compensation module can also be used in this role.

The goal of the receiver is to reconstruct the transmitted data symbols from the measured intensities $I^{(A)}(t) = |E^{(A)}(t)|^2$ and $I^{(B)}(t) = |E^{(B)}(t)|^2$. Clearly, when $|E_0|$ is large enough to guarantee the satisfaction of the minimum phase condition [4], the two fields can be uniquely reconstructed from the corresponding intensities [4]. What we show here is that when $|E_0|$ is reduced to the extent that the minimum phase condition is no longer satisfied, and the individual fields are no longer uniquely determined by their intensities [20], the data symbols can still be effectively extracted by imposing the requirement of consistency between the two measured intensity waveforms.

We assume that the photo-currents, which are equivalent to the intensity waveforms, are sampled at their Nyquist rate, which is equal to $2B$ (the intensity bandwidth), and that the processing is applied to blocks of N symbols at a time. The task of recovering the transmitted data can be expressed as a problem of finding the minimum of the following expression,

$$\{\hat{a}\}_{k=1}^{N} = \underset{z_k}{\text{argmin}} Q(\{z_k\}_{k=1}^{N}), \quad (3)$$

where

$$Q(\{z_k\}_{k=1}^{N}) = \sum_{m=0}^{2N-1} \left(\sqrt{I_m^{(A)}} - \left|A_m\left(\{z_k\}_{k=1}^{N}\right)\right|\right)^2 + \left(\sqrt{I_m^{(B)}} - \left|B_m\left(\{z_k\}_{k=1}^{N}\right)\right|\right)^2, \quad (4)$$

and where

$$A_m\left(\{z_k\}_{k=1}^{N}\right) = E_0 i^m e^{i\phi} + \sum_k z_k g\left(mT_s - kT\right) \quad (5)$$

$$B_m\left(\{z_k\}_{k=1}^{N}\right) = E_0 i^m e^{i\phi'} + \sum_k z_k g'\left(mT_s - kT\right), \quad (6)$$

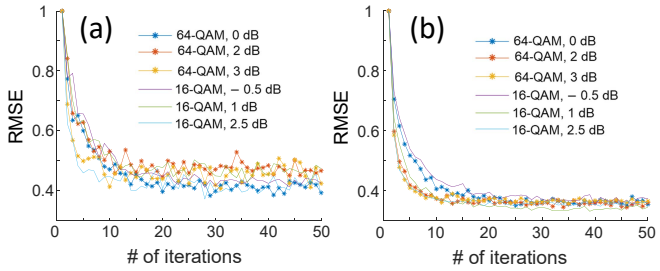

Fig. 2. The root-mean-square error of the recovered symbols as a function of the number of optimization iterations. Legends show modulation format and CSPR value. RMSE values are normalized to the result without optimization. (a) effective OSNR of 22 dB. (b) effective OSNR of 31 dB.

with $T_s = 1/2B$ being the sampling interval, and with $I_m^{(A,B)} = I^{(A,B)}(mT_s)$. Notice that the use of the amplitude as opposed to the square amplitude in Eq. (4), is not common, but as has been demonstrated in [19], it is advantageous in situations of the kind that we have here.

The process of finding the values of $\{z_k\}_{k=1}^N$ that minimize the expression in (4) is done by means of iterative optimization. This class of optimization problems has been studied extensively in multiple areas of research (see for example [12, 18], and references therein), and various algorithms for its solution have been proposed. In this work we use the Polak-Ribiere conjugate gradient method with the modified gradient expression of [19], whose details are discussed therein. Briefly put, the optimization procedure operates as follows. The first stage is to recover a rough estimate for the received signal by applying the standard KK algorithm to the received intensity samples $\{I_j^{(A)}\}_{j=1}^{2N}$, where $I_j^{(A)} = I^{(A)}(t = jT_s)$, and where N is the number of symbols in the processed frame [4]. Then, after dispersion compensation and removal of the CW carrier, an initial estimate for the data-symbols is generated $\{\hat{a}_m^{(0)}\}$ and fed into the optimization block (marked as OPT in Fig. 1). We stress that we implemented the algorithm of [19] as is, with the only difference being that we used it with the Polak Ribiere version of the conjugate gradient. The reason for adopting it was purely empirical, as it was found to perform better than all other algorithms that we have tried.

We considered 5 WDM channels spaced by 50 GHz, with 16 and 64 QAM modulated data at 32 Gbaud while using Raised-cosine pulses with a roll-off factor of 0.03. The link consisted of a 100-km span of standard single-mode fiber ($D = 17$ ps/nm/km, $\gamma = 1.3\,\mathrm{W}^{-1}\mathrm{km}^{-1}$, and attenuation of 0.2 dB/km), and the overall span-loss budget was 22 dB. As is usually the case in optically amplified transmission, we neglect thermal receiver noise and assume that the noise figure of the optical pre-amplifier is 5 dB. In all our simulations, the dispersive element placed in the lower branch in Fig. 1 produces chromatic dispersion of 340 ps/nm (equivalent to 20 km of SMF), except in Fig. 5, where this dispersion is varied. Each data-point is obtained by generating 70 independent frames of 2^{11} symbols, ensuring valid BER estimates in the relevant range of values.

In order to illustrate the efficiency of the optimization procedure, we show in Fig. 2 the root-mean-square (RMS) estimation error of the sample points, defined as $\sigma_{\mathrm{err}}^{(m)} = \sqrt{\mathbb{E}[(a_k - \hat{a}_k^{(m)})^2]}$, as a function of the number of optimization steps m, where $\mathbb{E}[\cdot]$ represents averaging with respect to the constellation symbols.

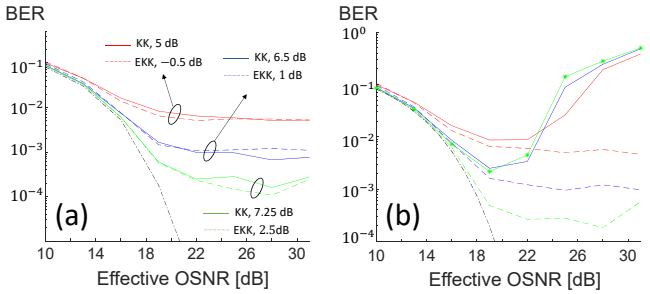

Fig. 3. BER vs. Effective OSNR for 16 QAM signal modulation in the cases of linear (a) and nonlinear (b) propagation. The dashed and solid curves correspond to EKK and KK, respectively. The legends in (a) show the CSPR in each of the cases and they apply also to plot (b). The dash-dotted curve is the theoretical curve of ideal coherent detection in back to back.

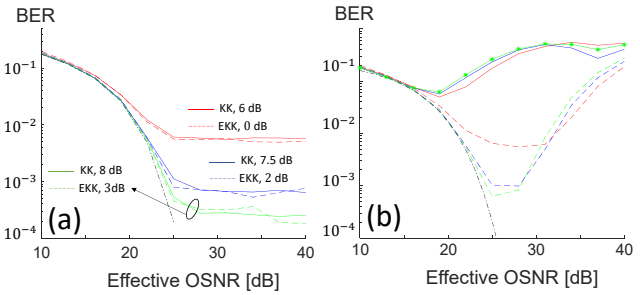

Fig. 4. Same as Fig. 3, but for 64 QAM.

The two panels shown in Fig. 2 were plotted for two different values of the effective optical signal-to-noise ratio (OSNR), which is defined as the OSNR that one would observe in the absence of the CW tone signal.[1] Figure 2a corresponds to a high effective OSNR of 31 dB where the errors are dominated by signal reconstruction. In Fig. 2b the effective OSNR is significantly lower (22 dB) and the errors (especially in the case of 64 QAM) are strongly affected by amplification noise. The various curves correspond to different CSPR values and modulation formats, as indicated in the figure. All curves were normalized to the error of the KK receiver which corresponds to the zeroth iteration. In all cases, good convergence is observed already after 10 iterations — a two orders of magnitude improvement relative to [15]. The improvement in the overall computational complexity is however only slightly bigger than one order of magnitude. That is because up to 10 evaluations of the gradient per iteration are required within the conjugate gradient method. In the results that are displayed in what follows we use 50 optimization steps in order to avoid possible dependencies of the optimization on operating conditions and to guarantee beyond doubt the integrity of the quantities that are being evaluated and compared. It must be noted that even this number of iterations is significantly smaller than in previously reported techniques [15–17].

Figure 3a shows the system BER as a function of the effective OSNR in the linear operation regime (i.e. with the value of γ artificially set to 0) in the case of 16 QAM modulation. Similarly to [4–6], consideration of the effective OSNR facilitates the comparison between the proposed schemes, the standard KK, and the

[1] We use the conventional definition of OSNR as the ratio between the average signal power and the noise power within a 12.5 GHz bandwidth.

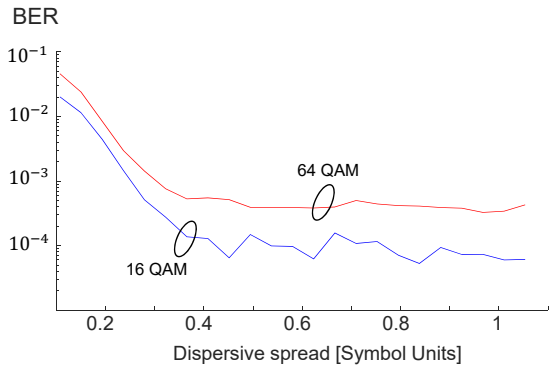

Fig. 5. BER vs. the dispersion of the dispersive module placed in the lower arm in the receiver in Fig. 1. The dispersive effect is quantified in terms of the dispersive spread of the signal in symbol units $\beta'' LB^2$. The curves are plotted for CSPR= 3 dB and for an effective OSNR of 25 dB without fiber nonlinearity.

ideal additive white Gaussian-noise (AWGN) channel. The solid lines show the KK results for CSPRs of 5 dB, 6.5 dB, and 7.25 dB. The dashed curves correspond to the EKK scheme and they show that the same performance as with KK can be obtained with CSPR values of −0.5 dB, 1 dB, and 2.5 dB, respectively. An advantage of 5.5 dB in the first two cases and an advantage of 4.75 dB in the third case. Figure 3b addresses the same scenario, but with the nonlinearity accounted for. Here, to change the effective OSNR, the launched signal power is changed, while keeping the noise power constant. The advantage of the reduced CSPR is clearly visible, as the performance of the EKK system is much less sensitive to nonlinear interference than the performance of KK, owing to the reduced CW power. Indeed, the case that is most affected by nonlinear distortions is the case with the highest CSPR (of 7.25 dB). The same picture is observed in the case of 64 QAM transmission, as illustrated in Fig. 4. In the case of linear transmission (Fig. 4a), the CSPR values are 6 dB, 7.5 dB, and 8 dB in the case of KK and the same respective BER performance levels are obtained with CSPR values of 0 dB, 2 dB, and 3 dB, with the EKK procedure — a CSPR gain of 5 dB to 6 dB in all cases. Once again, in the nonlinear propagation case, the advantage of the EKK scheme becomes even far more evident, as the nonlinear penalty associated with the high CW power carried by each of the WDM channels is avoided.

Finally, in Fig. 5 we examine the amount of chromatic dispersion used to decorrelate the intensities in the two branches of the receiver. Fixing the effective OSNR to 25 dB and the CSPR to 3 dB, we plot the resultant BER of the EKK receiver in the linear propagation regime, as a function of the dispersive spread $\beta'' LB^2$, where $\beta'' L$ is the accumulated dispersion of the decorrelating element. Interestingly, sufficient decorrelation occurs when the dispersive spread of the propagating waveform is of the order of 0.4 symbols, with no visible improvement that is observed for higher dispersion values.

To conclude, we have introduced and characterized the EKK receiver, which recovers complex-valued symbols from two direct detection measurements. The two directly measured signals differ only by the fact that one of them experiences a slightly higher chromatic dispersion than the other. With the proposed EKK scheme, the CW carrier power that is required for signal reconstruction is lower by 5 dB to 6 dB compared to the requirement of the regular KK scheme. The numerical search procedure was shown to reliably converge to the correct solution within a few tens of iterations, saving an order of magnitude in complexity relative to previously published results. Natural extensions of this work would be to explore the impact of imperfections in implementation and the effects of thermal receiver noise.

FUNDING INFORMATION

L. Blech and M. Shtaif acknowledge financial support from the Israeli Petacloud Consortium on Next Generation Hybrid Data Centers, as well as the support of the Israel Science Foundation Grant No. 1401/16. C. Antonelli and A. Mecozzi acknowledge financial support from the Italian Government under Cipe resolution n. 135 (Dec. 21, 2012), project INnovating City Planning through Information and Communication Technologies (INCIPICT), as well as under PRIN 2017 project Fiber Infrastructure for Research on Space-division multipled Transmission (FIRST).

DISCLOSURE

The authors declare no conflicts of interest.

REFERENCES

1. M. Schuster, S. Randel, C. A. Bunge, S. C. J. Lee, F. Breyer, B. Spinnler, and K. Petermann, IEEE Photon. Technol. Lett., 20, 670 (2008).
2. S. Randel, D. Pilori, S. Chandrasekhar, G. Raybon and P. Winzer, European Conference on Optical Communications (2015) pp. 1–3.
3. B. J. C. Schmidt, A. J. Lowery, J. Armstrong, J. Lightwave Technol. 26, 196 (2008).
4. A. Mecozzi, C. Antonelli, M. Shtaif, Optica, 3, 11, 1220, (2016)
5. Z. Li, M. S. Erkılınç; K. Shi, E. Sillekens, L. Galdino, B. C. Thomsen, P. Bayvel, R.I. Killey, J. of Lightwave Technol., 35, 10, 1887, (2017)
6. C. Antonelli, M. Shtaif, A. Mecozzi, Optical Fiber Communication Conference, (2017), paper Tu3I.5
7. X. Chen, C. Antonelli, S. Chandrasekhar, G. Raybon, A. Mecozzi, M. Shtaif, P. Winzer, European Conference on Optical Communications (2017), pp. 1–3.
8. Z. Li, M. S. Erkilinç, K. Shi, E. Sillekens, L. Galdino, B. C. Thomsen, P. Bayvel, R. I. Killey, European Conference on Optical Communications (2017), pp. 1–3.
9. Z. Li, M.S. Erkilinç, K. Shi, E. Sillekens, L. Galdino, B.C. Thomsen, P. Bayvel, R.I. Killey, European Conference on Optical Communications (2017), pp. 1–3.
10. S. Fan, Q. Zhuge, M. Y. S. Sowailem, M. Morsy-Osman, T. M. Hoang, F. Zhang, M. Qiu, Y. Li, J. Wu, and D. V. Plant, European Conference on Optical Communication (2017), pp. 1–3.
11. X. Chen, J. Cho, S. Chandrasekhar, P. Winzer, C. Antonelli, A. Mecozzi, and M. Shtaif, IEEE Photonics Conference (IPC) Part II (2017).
12. Y. Shechtman, Y. C. Eldar, O. Cohen, H. N. Chapman, J. Miao, and M. Segev, IEEE Signal Process. Mag. 32(3), 87, (2015).
13. A. Mecozzi, C. Antonelli, and M. Shtaif, Adv. Opt. Photon. 11, 480, (2019).
14. K. Huang, Y. C. Eldar, N. Sidiropoulos, IEEE Transactions on Signal Processing, 64, 6105 (2016).
15. L. Blech, Y. Eldar, C. Antonelli, A. Mecozzi, M. Shtaif, Optical Fiber Communication Conference (2018), paper Tu2D.7.
16. H. Chen, N. K. Fontaine, J. M. Gene, R. Ryf, D. T. Neilson, G. Raybon, arXiv:1903.02424 (2019).
17. H. Chen, H. Huang, N. K. Fontaine, R. Ryf, Opt. Lett., 45, 1188 (2020)
18. E. McLeod, A. Ozcan, Phys. Today, 70, 50 – 56 (2017).
19. G. Wang, G. B. Giannakis, Georgios, Y. C. Eldar, IEEE Transactions on Information Theory, 64, 773–794, (2018).
20. A. Mecozzi, M. Shtaif, Opt. Express, 26, 33970 (2018).

REFERENCES

1. M. Schuster, S. Randel, C. A. Bunge, S. C. J. Lee, F. Breyer, B. Spinnler, and K. Petermann, “Spectrally efficient compatible single-sideband modulation for OFDM transmission with direct detection," IEEE Photon. Technol. Lett., 20, 670–672 (2008).
2. S. Randel, D. Pilori, S. Chandrasekhar, G. Raybon and P. Winzer, “100-Gb/s discrete-multitone transmission over 80-km SSMF using single-sideband modulation with novel interference-cancellation scheme," European Conference on Optical Communications (2015) pp. 1–3.
3. B. J. C. Schmidt, A. J. Lowery, J. Armstrong, “Experimental Demonstrations of Electronic Dispersion Compensation for Long-Haul Transmission Using Direct-Detection Optical OFDM," J. Lightwave Technol. 26, 196–203 (2008)
4. A. Mecozzi, C. Antonelli, M. Shtaif, "Kramers-Kronig coherent receiver," Optica, 3, 11, 1220–1227, (2016)
5. Z. Li, M. S. Erkılınç; K. Shi, E. Sillekens, L. Galdino, B. C. Thomsen, P. Bayvel, R.I. Killey “SSBI mitigation and the Kramers–Kronig scheme in single-sideband direct-detection transmission with receiver-based electronic dispersion compensation," J. of Lightwave Technol., 35, 10, 1887–1893, (2017)
6. C. Antonelli, M. Shtaif, A. Mecozzi, “Kramers-kronig PAM transceiver," Optical Fiber Communication Conference, (2017), paper Tu3I.5
7. X. Chen, C. Antonelli, S. Chandrasekhar, G. Raybon, A. Mecozzi, M. Shtaif, P. Winzer, “4$\times$ 240 Gb/s dense WDM and PDM Kramers-Kronig detection with 125-km SSMF transmission," European Conference on Optical Communications (2017), pp. 1–3
8. Z. Li, M. S. Erkilinç, K. Shi, E. Sillekens, L. Galdino, B. C. Thomsen, P. Bayvel, R. I. Killey, “168 Gb/s/λ direct-detection 64-QAM SSB Nyquist-SCM transmission over 80 km uncompensated SSMF at 4.54 b/s/Hz net ISD using a Kramers-Kronig receiver," European Conference on Optical Communications (2017), pp. 1–3
9. Z. Li, M.S. Erkilinç, K. Shi, E. Sillekens, L. Galdino, B.C. Thomsen, P. Bayvel, R.I. Killey, “Joint optimisation of resampling rate and carrier-to-signal power ratio in direct-detection Kramers-Kronig receivers," European Conference on Optical Communications (2017), pp. 1–3
10. S. Fan, Q. Zhuge, M. Y. S. Sowailem, M. Morsy-Osman, T. M. Hoang, F. Zhang, M. Qiu, Y. Li, J. Wu, and D. V. Plant, “Twin-SSB direct detection transmission over 80km SSMF using Kramers-Kronig receiver,” European Conference on Optical Communication (2017) pp. 1–3.
11. X. Chen, J. Cho, S. Chandrasekhar, P. Winzer, C. Antonelli, A. Mecozzi, and M. Shtaif, “Single-wavelength, single-polarization, single-photodiode Kramers-Kronig detection of 440-gb/s entropy-loaded discrete multitone modulation transmitted over 100-km SSMF,” in IEEE Photonics Conference (IPC) Part II (2017).
12. Y. Shechtman, Y. C. Eldar, O. Cohen, H. N. Chapman, J. Miao, and M. Segev, “Phase retrieval with application to optical imaging: a contemporary overview," IEEE Signal Process. Mag. 32(3), 87-–109 (2015).
13. A. Mecozzi, C. Antonelli, and M. Shtaif, “Kramers-Kronig receivers," Adv. Opt. Photon. 11, 480–517 (2019).
14. K. Huang, Y. C. Eldar and N. Sidiropoulos, "Phase Retrieval from 1D Fourier Measurements: Convexity, Uniqueness, and Algorithms", IEEE Transactions on Signal Processing, vol. 64, issue 23, pp. 6105-6117, December 2016.
15. L. Blech, Y. Eldar, C. Antonelli, A. Mecozzi, M. Shtaif, “The enhanced Kramers Kronig receiver," Optical Fiber Communication Conference (2018), paper Tu2D.7.
16. H. Chen, N. K. Fontaine, J. M. Gene, R. Ryf, D. T. Neilson, G. Raybon, “Dual polarization full-field signal waveform reconstruction using intensity only measurements for coherent communications," arXiv:1903.02424 (2019).
17. H. Chen, H. Huang, N. K. Fontaine, R. Ryf, “Phase retrieval with fast convergence employing parallel alternative projections and phase reset for coherent communications," Opt. Lett., 45, 1188 (2020)
18. E. McLeod, A. Ozcan, “Microscopy without lenses," Phys. Today, 70, 50 – 56 (2017).
19. G. Wang, G. B. Giannakis, Georgios, Y. C. Eldar, “Solving systems of random quadratic equations via truncated amplitude flow, IEEE Transactions on Information Theory, 64, 773–794, (2018).
20. A. Mecozzi, M. Shtaif, “Coherent detection with an incoherent local oscillator," Opt. Express, 26, 33970 – 33981 (2018).